https://repository.uaeh.edu.mx/revistas/index.php/sahagun/issue/archive

Ingenio y Conciencia Boletín Científico de la Escuela Superior Ciudad Sahagún

Publicación semestral, Vol. 12, No. 23 (2025) 85-91

ISSN: 2007-784X

Modelos matemáticos que describen la electrofisiología de las células trabeculares humanas en cultivo celular

Mathematical models describing the electrophysiology of human trabecular cells in cell culture

Jorge Santiago Amaya [a], Kevin A. Aguilar Bailón [b]

Abstract:

This paper describes two mathematical models that define the behavior of trabecular cells. These models were built from image fragments presenting the electrophysiological response of the trabecular meshwork. The first model refers to the behavior of the voltage-dependent ion channel Ca^{2+} in the presence of Barium $Ba^{2+}$and tetrodotoxin TXT, the second defines the states of deporalization, reporalization and hyperporalization when NA does not exist in the extracellular medium. These models are based on work done by Albrecht Lepple-Wienhues on human trabecular meshwork cells.

Keywords:

Glaucoma, extracellular medium, trabecular cells, stimulating the cornea with specific electric fields

Resumen:

Este artículo describe dos modelos matemáticos que definen el comportamiento de las células trabeculares. Estos modelos se construyeron a partir de fragmentos de imágenes que presentan la respuesta electrofisiológica de la malla trabecular. El primer modelo se refiere al comportamiento del canal iónico dependiente de voltaje Ca^{2+} en presencia de Ba^{2+} de Bario y tetrodotoxina TXT, el segundo define los estados de deporalización, reporalización e hiperporalización cuando no existe NA en el medio extracelular. Estos modelos se basan en los trabajos realizados por Albrecht Lepple-Wienhues en células humanas de la malla trabecular.

Palabras Clave:

Glaucoma, medio extracelular, células trabeculares, estimulación de la córnea con campos eléctricos específicos

Introduction

Glaucoma is a medical term that describes a group of progressive optic neuropathies characterized by degeneration of retinal ganglion cells and causing changes in the optic nerve head (Harasymowycz et al., 2016). There are two types of this pathology, primary and secondary, at the same time two subcategories, open and closed angle (Alisson et al., 2020). This depends on your anatomy and the underlying pathophysiology. Glaucoma is associated with increased intraocular pressure that evokes optic nerve damage (Khaled et al., 2017). intraocular pressure (POI) is determined by the volume of aqueous humor in its anterior and posterior chambers (Cerro, 2005). In the case of open angle glaucoma, in most cases the increase in eyeball pressure is associated with poor functioning of the trabecular meshwork, specifically in the Schlemm chamber (Cela et al., 2021). In it, when the cells have a sufficiently large volume, the flow of aqueous humor decreases and evokes an increase in internal pressure of the eye. When the volume of the cells of the trabecular meshwork decreases, this

[a] Autor de Correspondencia, Tecnológico Nacional de México | Tecnológico de Estudios Superiores Chalco | Chalco-Estado de México | México, https://orcid.org/0000-0003-3432-4305, Email: jorge_sa@tesch.edu.mx

[b] SYS-DT S.A. de C.V., | Estado de México | México, https://0000-0001-9516-9025, Email: kevenidos@hotmail.com

Fecha de recepción: 24/10/2024, Fecha de aceptación: 06/11/2024, Fecha de publicación: 05/01/2025

DOI: https://doi.org/10.29057/escs.v12i23.14020

pressure is released by allowing the aqueous humor to pass through the Schlemm chamber. This balance can be altered for different reasons, including poor functioning of trabecular cells by tyrosine kinases [Kaufman, 2005]. In equivalence, these cells altered by these molecules have a different electrophysiological response to healthy cells (Machemer, 1988).

There are around 76 million people worldwide who suffer from glaucoma, of which it is estimated that 57.5 million cases are Primary Open Angle Glaucoma (POAG). The number of people with glaucoma is expected to reach 111.8 million by 2040 (Allisson, et al., 2020). Open Angle Glaucoma is most common after age 40 and affects approximately one percent of the world's population (Abu-Amero et al., 2017). There is currently no cure because dying retinal neurons do not regenerate; however, disease progression can be slowed with drugs that lower IOP (Flaxman et al., 2017). People with progressive glaucoma encompass different categories of patients, from those who are untreated because they are unaware of the disease to those who do not have access to treatment; and others who are noncompliant with treatment to those who progress despite treatment (Abe et al., 2016).

The socioeconomic impact of glaucoma in the United States

One study estimated that more than 2.2 million Americans have glaucoma, but only half know they have it. Glaucoma is the second leading cause of blindness in African Americans; blindness is 6 to 8 times more common in African Americans than in Caucasians (Cogdon at al. 2004).

The U.S. National Institutes of Health (NIH) in 1997 noted that more than 120,000 people are blind due to glaucoma, accounting for 9% to 12% of all cases of blindness. The Glaucoma Research Foundation on its website defines glaucoma as responsible for more than 10 million visits to physicians every year (Quigley et al., 1997).

The cost to the U.S. government exceeds $1.5 billion annually (NEI, 1998) for health care expenses related to this disease.

The socioeconomic impact of glaucoma in Mexico

Martínez et al., conducted a study to estimate the direct and indirect costs generated by POAG in Mexican society due to the complexity of diagnosing and treating glaucoma. This study classified direct costs (costs assumed by people with POAG) and indirect costs (costs assumed by Mexican society). The total sum of direct and indirect costs annually in Mexico in 2016 was approximately $21,237,417,389.57 pesos, and at 5 years $94,427,184,459.98 pesos (Martínez et al., 2016), see table 1.

Table 1. Estimation of the direct and indirect costs in pesos (MXN) generated by GPAA in Mexican society in 2016

Cost	**1-year amount**	**5-year amount**
Direct cost	$16,466.52	$65,670.38
Indirect cost	$9,615,633,309.66	$48,078,166,548.29
Total cost	$21,237,417,389.57	$94,427,184,459.98

For this reason, the understanding of the electrophysiology of trabecular cells is of vital importance to understand in detail the causes of GAAP so that in the future different alternatives are proposed to treat this pathology.
In the present work we propose mathematical models that describe the electrophysiological response of cell cultures of the human trabecular meshwork. These models are based on studies by Albrecht Lepple-Wienhues et al (1994). His research consists of seven different cell culture lines. These lines were obtained using human tissue from four different eyes. Table 1 shows the different studies carried out by Albrecht Lepple-Wienhues et al. (1994), in their cell culture lines.

Table 2. General description of the different numbers of experimentation carried out on the cell culture lines of the human trabecular meshwork.

Cell Line	Ba^{2+}	Na^{+} Removal	Acetyl-choline	Isopro-terenol	Endo-thelin
BR 5	4	16	8	27	8
BER 5 SV40	3	-	-	3	-
ALC 4.1	10	1	-	-	-
ALC 4.2	3	-	-	-	-
ALC 10.1	21	11	8	7	4
ALC 10.2	12	-	-	-	-
ALC 2.1	4	8	1	3	-
ALC 2.2	6	18	6	15	9
TOTAL	63	54	23	55	21

Methodology

From the studies carried out by Lepple-Wienhues et al. (1994), the electrophysiological responses of trabecular cells were analyzed through the algorithm proposed by Santiago J et al [6]. Next, the procedures carried out to determine the mathematical models that establish the behavior of the membrane potential when Barium Ba^(2+), tetrodotoxin TTX are introduced into the extracellular medium and the elimination of sodium in the extracellular medium Na^(2+).

Barium 〖Ba〗^(2+) and Tetrodotoxin TTX

Lepple-Wienhues et al. (1994), published the change in membrane potential when applying barium 〖Ba〗^(2+)in their cell culture line ALC 4.1, this phenomenon can be seen in figure 1-a. From the graph reported by Lepple-Wienhues et al. (1994), a fragment of the signal that defines the behavior of the membrane potential evoked by voltage-gated calcium 〖Ca〗^(2+)channels was taken, figure 1-b to describe the model. mathematical model of these channels evoked by Barium Ba and Tetrodotoxin TTX, equation 1.

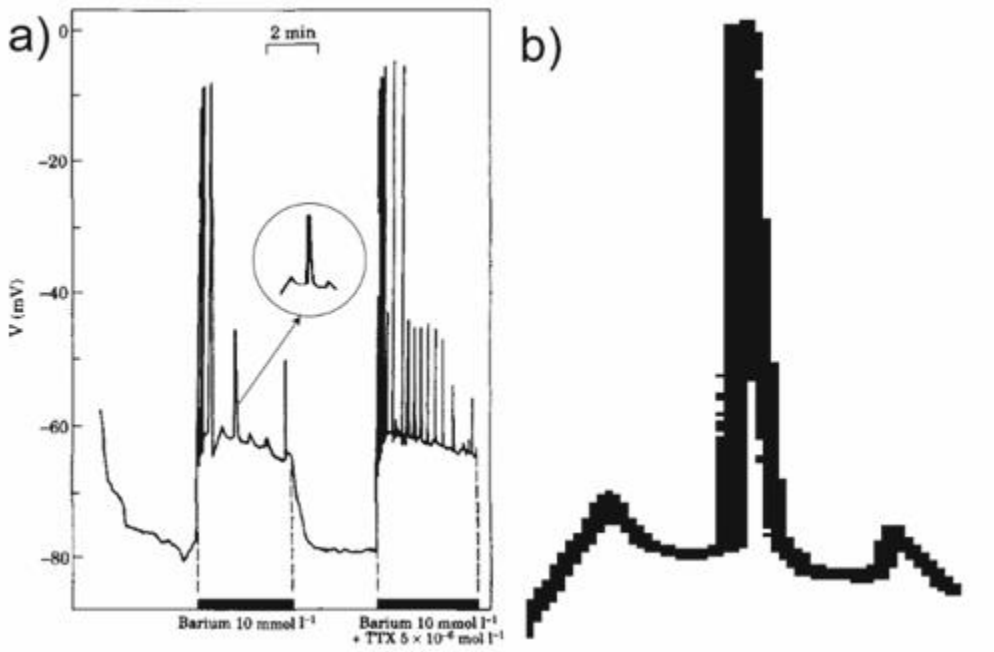

Figure 1 Diagram of the behavior of the voltage-gated channels by Barium Ba and Tetrodotoxin TTX. a) Graph reported by Lepple-Wienhues et al. (1994). b) fragment obtained on the electrophysiological response on the behavior of voltage-dependent AC channels.

Depolarization repolarization and hyperpolarization

Lepple-Wienhues et al [5], in their cell culture lines ALC 2.2, 2.1, 10.1 and BER 5 (n = 54), removed Na^{2+}in their extracellular medium to find the behavior of the membrane potential in endothelial and muscle cells. ciliary, its representation can be seen in Figure 2. From their reported study, a fraction was used to determine the mathematical model of depolarization (equation 3), repolarization (equation 4), and hyperpolarization (equation 5) of these cells. The set of these three states is represented in equation 2.

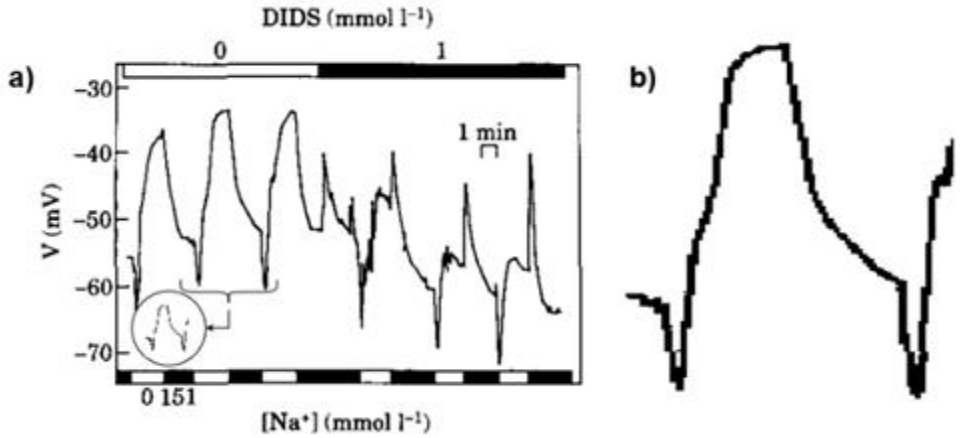

Figure 2 Scheme that describes the behavior of the membrane potential when 〖Na〗^(2+)is eliminated in the extracellular medium. a) Graph reported by Lepple-Wienhues et al. (1994). b) fragment of the electrophysiological response of the membrane potential.

$$f_m(t) = \begin{cases} -25.75 * e^{-0.05607*t+0.393} - 37.25 & 0.0 < t < 94.28\ s \\ 16.833 * e^{-0.04081*t+3.9} - 55.33 & 94.28 < t < 218.57\ s \\ 7.66 * e^{-0.22435*t+49.042} - 63 & 218.57 < t < 240\ s \end{cases} \quad (1)$$

$$v_m(t) = -25.75 * e^{-0.05607*t+0.393} - 37.25 \qquad 0.0 < t < 94.28\ s \quad (2)$$

$$v_m(t) = 16.833 * e^{-0.04081*t+3.9} - 55.33 \qquad 94.28 < t < 218.57\ s \quad (3)$$

$$v_m(t) = 7.66 * e^{-0.22435*t+49.042} - 63 \qquad 218.57 < t < 240\ s \quad (4)$$

$$v(t) = \begin{cases} 0.023 * e^{13.5654*t} & 0.0 < t < 0.368\ s \\ 2.067 * (e^{-25.0961549*t+9.25} - 1) + 3.4 & 0.368 < t < 0.4283\ s \\ 0.099 * e^{71.703*t-30.7142} + 1.8 & 0.4283 < t < 0.4980\ s \\ 15.134 * \left(e^{(-50.1923)(t)+(25.0)} - 1\right) + 16.47 & 0.4980 < t < 0.5977\ s \\ 0.0071 * e^{(125.4808)(t)+(-75.0000)} + 1.3 & 0.5977 < t < 0.6375\ s \\ 2.34 * e^{(-25.0961)(t)+(16.0)-1} + 2.4 & 0.6375 < t < 0.8367\ s \end{cases} \quad (5)$$

RESULTS

Voltage Dependent Ca^{2+}Channel

From equation 1, a mathematical model represented by Figure 3 was established. This forms the behavior of the membrane potential when the voltage-dependent Ca^{2+}channels are activated by the presence of barium $Ba^{2+}$and TetrodotoxinTTX. This equation was coupled to generate the mathematical expressions described in tables 1a, 1b, 1c, 1d, 1e, 1f. The way to couple this function was through its repetition, its displacement, as well as the change of its amplitude.

Table 2a. Mathematical model of the behavior of the Channels depending on the voltage

Number	Time function F(t)	t intervals
1	-80	0.0<t<282.45s
2	$0.3755 * e^{(0.51226*t-142.0409)} - 64.3241$	282.45s<t<287.36s
3	$57.5067 * e^{(-0.3585*t+102.9286)} - 59.9334$	287.36s<t<300.87s
4	$0.3755 * e^{(0.4845*t-151.1615)} - 63.2000$	300.87s<t<322.61s
5	$71.8834 * e^{(-0.3391*t+109.3130)} - 74.3101$	322.61s<t<336.89s
6	$2.0666656 * e^{(-0.1569*t+55.9188)} - 61.6667$	336.89s<t<374.03s
7	$0.1423 * e^{(0.4481*t-164.0538)} - 62.8221$	374.03s<t<377.54s
8	$15.1333 * e^{(-0.3137*t+25.5834)} - 61.8663$	377.54s<t<393.68s

Table 2b. Mathematical model of the behavior of the Channels depending on the voltage

Number	Time funcion F(t)	t intervals
9	$0.007187136 * e^{(0.7794*t-308.3442-308.3442)} - 61.66$	393.68s<t<401.79s
10	$(1 * 2.3999) * e^{(-0.1559*t+62.6688)} - 62.9999$	401.79s<t<419.44s
11	$0.0069 * e^{(13.565488*\left(\frac{t}{161}\right)-32.9017)} - 63$	419.44s<t<448.39s
12	$1.44 * e^{((-0.1559*t)+69.9341)} - 63.9999$	448.39s<t<466.05s
13	$0.0069 * e^{(0.0843*t-36.7693)} - 64$	466.05s<t<494.29s
14	$(1.55 * 0.1976) * e^{(0.4454*t-215.3216)} - 65.6443$	494.29s<t<492.88s
15	$-0.022909 * e^{(0.0843*t-39.0306)} - 62$	492.88s<t<510.53s
16	−80	510.53s<t<723.08s

Table 2c. Mathematical model of the behavior of the Channels depending on the voltage.

Number	Time funcion F(t)	t intervals
17	$0.3755 * e^{(2.8681*t-44058)} - 69.7590$	723.08s<t<723.15s
18	$57.5067 * e^{-2.0076t-10173.4421} - 461.9334$	723.15s<t<725.57s
19	$0.3755 * e^{2.8661t-2078.4027} - 65.3241$	725.57s<t<726.44s
20	$57.5067 * e^{-2.0076t+1458.3816} - 60.9334$	726.44s<t<728.85s
21	$0.3755 * e^{2.8681t-2087.83889} - 64.3241$	728.85s<t<729.73s
22	$57.5067 * e^{-2.0076t+1464.9869} - 59.9334$	729.73s<t<732.14s
23	$0.1689 * e^{1.5934t-1171.5094} - 61.9458$	732.14s<t<738.44s
24	$028.878 * e^{-1.1153t+825.7871} - 59.9695$	738.44s<t<748.93s
25	-60	748.93s<t<748.64s
26	$0.41305 * e^{2.8681t-2142.9357} - 64.02$	748.64s<t<748.94s

Table 2d. Mathematical model of the behavior of the Channels depending on the voltage.

Number	Time funtion F(t)	t intervals
27	$63.25737 * e^{-2.0076t+1503.5547} - 63.6840$	748.94s<t<751.35s
28	$1.8599 * e^{-1.0038t-759.4903} - 61.4999$	751.35s<t<759.32s
29	$0.41305 * e^{2.8681t-2197.2079} - 78.10431$	759.32s<t<767.86s
30	$61.137638 * e^{-2.0076t+1541.5452} - 62.8663$	767.86s<t<773.46s
31	$0.14269 * e^{1.0243t-789.1682} - 64.4431$	773.46s<t<775.43s
32	$21.8525 * e^{-0.7170t+555.9176} - 62.7746$	775.43s<t<782.19s
33	$1.6532 * e^{-0.7170t+560.7612} - 62.3559$	782.19s<t<793.85s
34	$0.1464 * e^{1.0243t-810.2346} - 66.0863$	79385s<t<796.00s
35	$22.4276 * e^{-0.71703t+570.6641} - 64.374$	796.00s<t<811.97s

Table 2e. Mathematical model of the behavior of the Channels depending on the voltage.

Number	Time funtion F(t)	t intervals
36	$0.1464 * e^{1.0243t-828.7914} - 66.0863$	811.97s<t<814.12s
37	$22.4276 * e^{-0.7170t+583.6503} - 64.3740$	814.12s<t<820.87s
38	$0.1502 * e^{0.9958t-822.0844} - 65.72964$	820.87s<t<830.68s
39	$23.0026 * e^{-0.6971t+578.9841} - 63.97336$	830.68s<t<837.63s
40	$0.1502 * e^{0.8852t-744.5995} - 66.72964$	837.63s<t<846.94s
41	$23.00268 * e^{-0.619658t+78.5657} - 64.97336$	846.94s<t<854.76s
42	$0.12767 * e^{0.8744t-750.2210} - 66.870194$	854s<t<863.83s

Table 2f. Mathematical model of the behavior of the Channels depending on the voltage.

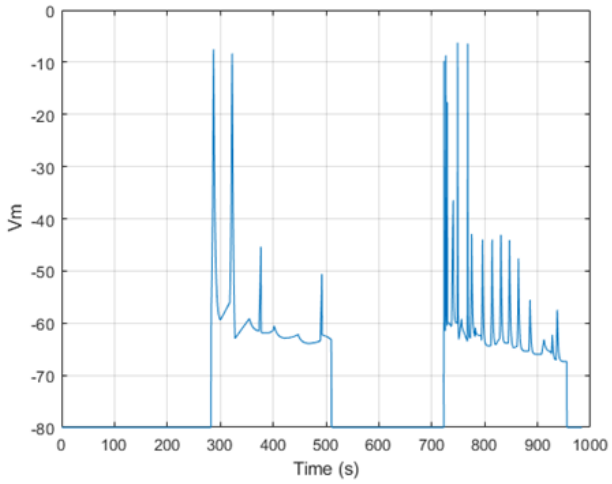

Figure 3. Graphic representation of the mathematical model of tables 1a, 1b, 1c, 1d, 1e, 1f. This scheme represents the behavior of the 〖Ca〗^(2+)channels in the presence of 〖Ba〗^(2+)and TTX.

Number	Time funtion F(t)	t intervals
43	$19.5522 * e^{-0.6121t+528.6556} - 65.3773$	863.83s<t<882.89s
44	$0.0751 * e^{0.8744t-769.4030} - 66.8648$	882.89s<t<885.77s
45	$11.50134 * e^{-0.6121t+542.0810} - 65.98668$	885.77s<t<908.07s
46	$1.8599 * e^{-0.30605t+279.3618} - 65.4999$	908.07s<t<926.09s
47	$0.03755 * e^{0.8744t-805.4356} - 67.28821$	926.09s<t<927.89s
48	$5.45067 * e^{-0.6121t+567.8648} - 64.18663$	927.89s<t<935.44s
49	$0.0751 * e^{0.87443048t-814.41701834} - 67.56442$	935.44s<t<937.24s
50	$10.90134 * e^{-50.1923t+16492.2102} - 67.37326$	937.24s<t<955.58s
51	-80	955.58s<t<984.00s

Depolarization repolarization and hyperpolarization

In the simulation of the membrane potential, the inhibitor diisothiocyanostilbene DIDS reported by Lepple-Wienhues et al. (1994) was eliminated, to establish the natural behavior of trabecular cells in different stages of cellular metabolism. The signal of equation 2 was shifted in time and a periodic signal was defined according to the same equation, this behavior is described in Figure 5, its mathematical expression is defined in equation 6.

$$v_m(t) = \sum_{n=0}^{3} f_m(t - n * t_0)\, t_0 = 240\ s \qquad (6)$$

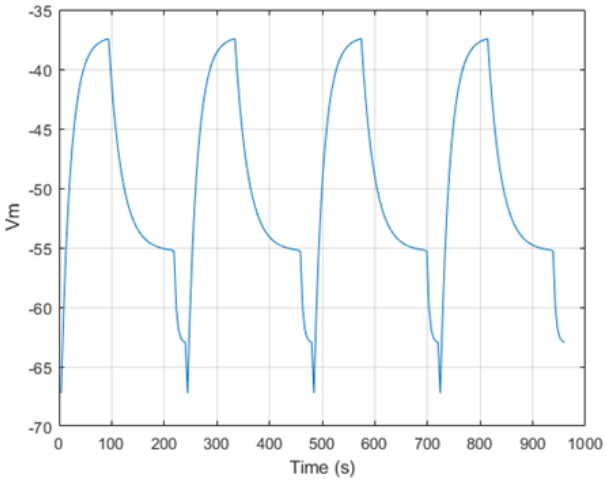

Figure 4. Graphical representation of the mathematical model constituted by equation 6 that refers to the behavior of the membrane potential in a periodic way.

Conclusion

From the equations proposed in this work, the probability function in which voltage-gated ion channels $Ca^{2+}$are activated in the presence of $Ba^{2+}$and $TTX$was defined. This mathematical model gives an approximation of the real biological behavior, however, it does not guarantee the correct prediction of the behavior of these channels in vivo. The justification is based on the fact that these cell cultures have controllable environmental conditions, while in vivo this is not the case (Eugene, 2005). Another relevant result is the behavior of the membrane potential in trabecular cells, as shown in Figure 4. Whose functions are characterized by a set of exponential expressions that mark the behavior of an RC circuit, where in the repolarization state, it can be equivalent to a capacitor in charging phase, while repolarization a capacitor in discharging phase, and the same as hyperpolarization, but with even more negative values. These states indicate a constant cycle of behavior that determines cellular metabolism (Hammond, 2001).

Discussion

Although in the present work a set of mathematical equations is exposed that describes the behavior of the cell membrane in its three states, this does not determine that these equations definitively mark the behavior of the endothelial cells and the ciliary muscle. The foundation of this statement is in the non-linear mechanism that a cell has to comply with its cellular metabolism (Eugene, 2005). This fact can be verified by the application of endotein in the cell lines ALC 2.2, 10.1 and VER 5, see Figure 5, where the physiological response is represented by equation 7 and shown in Figure 6. However, the most accurate way of predicting the membrane potential is given by equation 2. The justification is given in the experimentation of this behavior by eliminating it in its extracellular medium, since there is no other substance that alters its behavior. These mathematical equations could be the object of study to thoroughly understand the behavior of the cells of the trabecular meshwork, in addition to defining new alternatives in treatments for the control of IOP, an example of this is the proposal by Luis Niño et al. (2018), whose method is based on stimulating the cornea with specific electric fields. This type of treatment can be monitored through a system as defined by Amaya J. et al. (2021), where the mean square error is used to verify the correct application of electrical stimuli to the cornea.

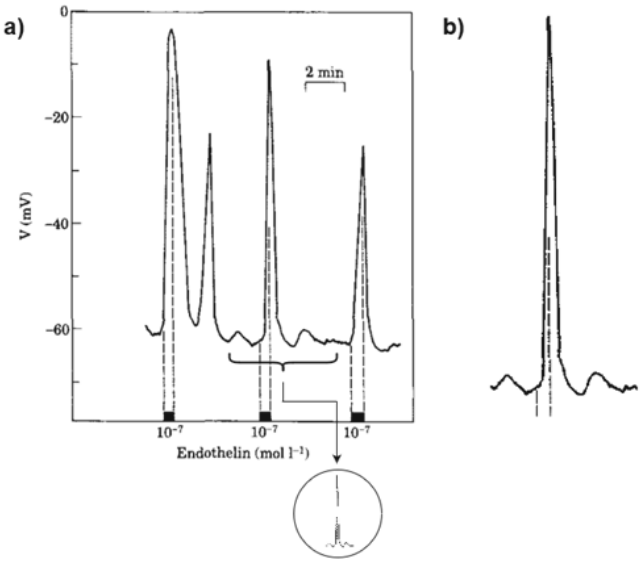

Figure 5. Scheme that describes the behavior of the membrane potential when entering endothelin. a) Graph reported by Lepple-Wienhues et al. (1994). b) fragment of the electrophysiological response of the membrane potential.

$$v_m(t) = \begin{cases} -2.7084 * e^{-0.1310*t+0.8929} - 57.2916 & 0.0 < t < 47.72\ s \\ 2.22 * e^{-0.0991*t+4.7276} - 60 & 47.72 < t < 95.45\ s \\ 0.3397 * e^{0.1111*t-10.907} - 60.1177 & 95.45 < t < 143.18\ s \\ -0.296 * e^{0.7143*t-14.9988} - 9.458 & 143.18 < t < 190.91\ s \\ 2.96 * e^{-0.1467*t+28} - 60.74 & 190.91 < t < 225\ s \\ -2.96 * e^{-0.0991*t+22.29} - 57.04 & 225 < t < 252.27\ s \\ -0.0141 * e^{0.0852*t-20} - 57.04 & 252.27 < t < 300\ s \end{cases} \quad (7)$$

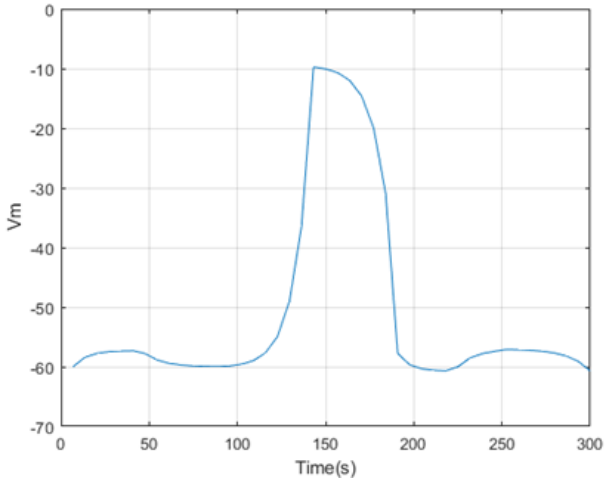

Figure 6. Graphical representation of the mathematical model represented by equation 7. This model represents the membrane potential when endothelin is introduced into the cell medium.

Another relevant piece of information from this study is the behavior of the voltage-dependent channels, since from a single fragment of the signal (equation 2) it was possible to determine the behavior of these channels in two different substances (Barium Ba and Tetrodotoxin TTX), therefore, this sets the standard for having a little more certainty about the probability in which the channels are activated, therefore these equations could be used to simulate certain behaviors of this ion channel.

Referencias

Abe, R. Y., Diniz-Filho, A., Costa, V. P., Gracitelli, C. P., Baig, S., & Medeiros, F. A., (2016). The impact of location of progressive visual field loss on longitudinal changes in quality of life of patients with glaucoma. *Ophthalmology*, *123*(3), 552-557.

Allison, K., Patel, D., &Alabi, O., (2020). Epidemiology of glaucoma: The past, present, and predictions for the future. Cureus, 12(11).

Amaya, J., González, C. and Bailon, K., (2021). Web Control System for Transcorneal Electric Stimulation Devices. Journal of Biomedical Science and Engineering, 14, 452-459. doi: 10.4236/jbise.2021.1412039.Practice. Publicación anticipada en línea. doi:10.1 057/palgrave.kmrp.8500141.

Cela, D., Brignole-Baudouin, F., Labbé, A., & Baudouin, C., (2021). The trabecular meshwork in glaucoma: An inflammatory trabeculopathy?. Journal Français d'Ophtalmologie, 44(9), e497-e517.

Cerro, D. S., (2005). Implicaciones funcionales de la señalización purinérgica en la red trabecular. Tesis Doctoral, Universitat de Barcelona, Departament de Ciències Fisiològiques I. Barcelona.

Eugene, M. I., (2005). The Neurosciences Institute. Dynamical Systems in Neuroscience: The Geometry of Excitability and Bursting. The MIT Press. ISBN-13: 978-0262090438, ISBN-10: 0262090430

Gil-Carrasco, F., Ochoa-Contreras, D., Torres, M.A., Santiago-Amaya, J., Pérez-Tovar, F.W., González-Salinas, R. and Niño-de-Rivera, L., (2018). Transpalpebral Electrical Stimulation as a Novel Therapeutic Approach to Decrease Intraocular Pressure for Open-Angle Glaucoma: A Pilot Study. Journal of Ophtalmology, Article ID: 2930519. https://doi.org/10.1155/2018/2930519 https://pubmed.ncbi.nlm.nih.gov/30116627

Hammond, C., (2001). Cellular and Molecular Neurobiology. 2nd Edition, Academic Press, Oxford.

Harasymowycz, P., Birt, C., Gooi, P., Heckler, L., Hutnik, C., Jinapriya, D., ... & Day, R. (2016). Medical management of glaucoma in the 21st century from a Canadian perspective. *Journal of ophthalmology*, *2016*(1), 6509809.

Kaufman, P. L. (2005). Changes in aqueous humor dynamics with age and glaucoma. *Progress in retinal and eye research*, *24*(5), 612-637.

Khaled k Abu-Amero, PhD FRCPath and Deepak P Edward, MD. Primary Congenital Glaucoma, (2017). Medline Plus by National Library of Medicine.

Lepple-Wienhues, A., Rauch, R. Clark, A. F., Grássmann, A., Berweck, S., Wiederholt, M., (1994). Electrophysiological Properties of Cultured Human Trabecular Meshwork Cells, Experimental Eye Research, Volume 59, Issue 3, Pages 305-311, ISSN 0014-4835, https://doi.org/10.1006/exer.1994.1112.

Machemer, H., (1988). Electrophysiology. *Paramecium*, 185-215.

Santiago, J., Romero, C., Guerrero, S., Trejo, F. and Robles, D., (2021). Bio-Informatic Model of Tyrosine Kinases Inhibitors in Trabecular Meshwork Cells. New Trends in Intelligent Software Methodologies, Tools and Techniques, Vol. 337, 351-358. https://doi.org/10.3233/FAIA210034.